

000

054

001

055

002

056

003

057

004

058

005

059

006

060

007

061

Xuan Cao Zhang Chen Anpei Chen Xin Chen Shiying Li Jingyi Yu

062

ShanghaiTech University

063

393 Middle Huaxia Road, Pudong, Shanghai, China

064

{caoxuan, chenzhang, chenap, chenxin2, lishy1, yujingyi}@shanghaitech.edu.cn

065

012

066

013

067

014

068

015

069

016

070

017

071

018

072

019

073

020

074

021

075

022

076

023

077

024

078

025

079

026

080

027

081

028

082

029

083

030

084

031

085

032

086

033

087

034

088

035

089

036

090

037

091

038

092

039

093

Noise on Normal (°)	Mean Angular Error (°)		Mean Relative Absolute Error (%)	
	w/o AO	w/ AO	w/o AO	w/ AO
2.5	5.23	1.70	5.54	4.07
5	7.09	1.89	7.45	4.87
7.5	8.41	2.66	8.78	5.43
10	13.91	6.17	12.36	5.99
15	23.54	6.92	19.45	7.19
Proxy Model	10.99	3.55	11.94	4.74

049

094

050

095

051

096

052

097

053

098

Supplementary Material for Sparse Photometric 3D Face Reconstruction Guided by Morphable Models

Xuan Cao Zhang Chen Anpei Chen Xin Chen Shiying Li Jingyi Yu

062

ShanghaiTech University

063

393 Middle Huaxia Road, Pudong, Shanghai, China

064

{caoxuan, chenzhang, chenap, chenxin2, lishy1, yujingyi}@shanghaitech.edu.cn

065

1. Additional Evaluations

1.1. Proxy Face Model Generation

With the rapid progress of learning-based model-from-image approaches, we have also tried a state-of-the-art learning-based method [3] to generate proxy face model. However, it sometimes exhibits significant misalignment as shown in the second and fourth rows of Fig. 1, which degrades our final face reconstruction. As a result, we choose to use PCA-based 3D morphable model [1] due to its stable prediction quality for images captured in our setup, as shown in the first and third rows of Fig. 1.

1.2. Light Calibration Accuracy

We evaluate the accuracy of our light calibration approach and show that it can correctly estimate positions and illumination of light sources under inaccurate initial normals. Using face model from [2], we render 5 images illuminated by different near point light sources. The illumination and distance of light sources vary up to 10%. A proxy face model is predicted using [1].

As shown in Table 1, we analyze calibration accuracy under different initial normals. To get initial normals, we add noise on groundtruth normals so that they are randomly deviated by certain angles. We also compare the accuracy with and without the alternating optimization step introduced in our paper. To measure accuracy, we compute mean angular error of per-pixel light directions and mean relative absolute error of scaled per-pixel light directions. For each scaled per-pixel light direction, its relative absolute error is computed as the L1 norm of the difference with its groundtruth counterpart divided by the L2 norm of the groundtruth scaled per-pixel light direction. As a reference, the parallel light directions computed from groundtruth albedo and normal have a mean angular error of 6.17° and mean relative absolute error of 6.52%. Table 1 shows that when initial normals are not far from the correct ones, our calibration approach can effectively compensate for the inaccuracy of initial normals after applying alternating optimization. The last row in the table shows the calibration accuracy obtained by utilizing the initial normals from proxy face model.

Table 1: The accuracy of our light calibration method with and without alternating optimization (AO) under different initial normals.

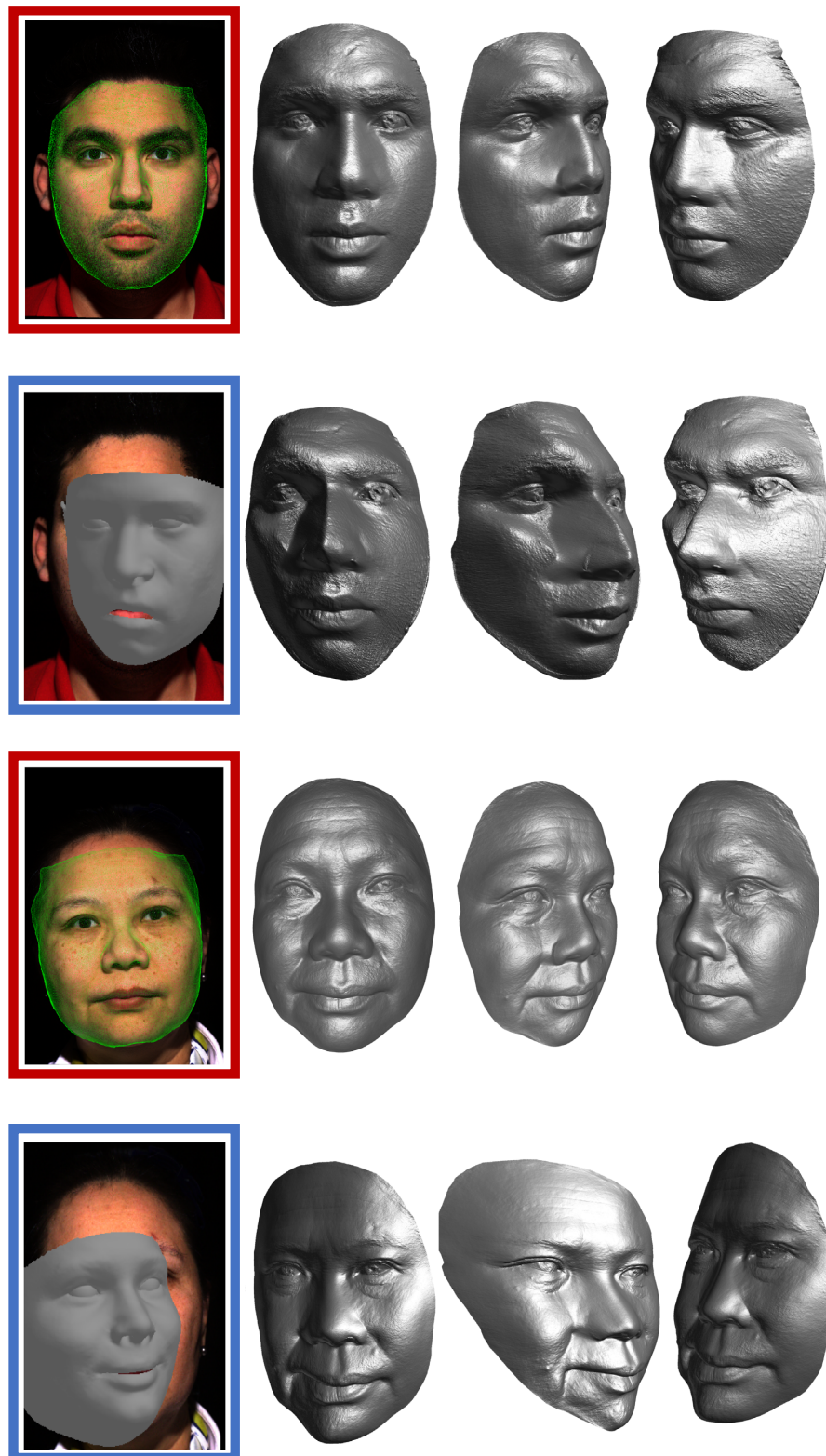
108
109
110
111
112
113
114
115
116
117
118
119
120121
122
123
124
125
126
127
128
129
130
131
132133
134
135
136
137
138
139
140
141
142
143
144145
146
147
148
149
150
151
152
153
154
155
156
157158
159
160
161162
163
164
165
166
167
168
169
170
171
172
173
174175
176
177
178
179
180
181
182
183
184
185
186187
188
189
190
191
192
193
194
195
196
197
198
199200
201
202
203
204
205
206
207
208
209
210
211
212
213
214
215

Figure 1: Comparison of proxy face models using [1, 3] and corresponding reconstruction results. The first column is proxy face models using [1, 3]. The second to fourth columns are our reconstructed face models using corresponding proxy face models in the first column.

216	References	270
217		271
218	[1] P. Huber, G. Hu, R. Tena, P. Mortazavian, P. Koppen, W. J. Christmas, M. Ratsch, and J. Kittler. A multiresolution 3d morphable face model and fitting framework. In <i>Proceedings of the 11th International Joint Conference on Computer Vision, Imaging and Computer Graphics Theory and Applications</i> , 2016. 1, 2	272
219		273
220	[2] W. C. Ma, T. Hawkins, P. Peers, C. F. Chabert, M. Weiss, and P. Debevec. Rapid acquisition of specular and diffuse normal maps from polarized spherical gradient illumination. In <i>Eurographics Conference on Rendering Techniques</i> , pages 183–194, 2007. 1	274
221		275
222	[3] A. Tuan Tran, T. Hassner, I. Masi, and G. Medioni. Regressing robust and discriminative 3d morphable models with a very deep neural network. In <i>IEEE Conference on CVPR</i> , July 2017. 1, 2	276
223		277
224		278
225		279
226		280
227		281
228		282
229		283
230		284
231		285
232		286
233		287
234		288
235		289
236		290
237		291
238		292
239		293
240		294
241		295
242		296
243		297
244		298
245		299
246		300
247		301
248		302
249		303
250		304
251		305
252		306
253		307
254		308
255		309
256		310
257		311
258		312
259		313
260		314
261		315
262		316
263		317
264		318
265		319
266		320
267		321
268		322
269		323